PAPER

Kinks in experimental diffusion profiles of a dissolving semi-crystalline polymer explained by a concentration-dependent diffusion coefficient

Helen E. Hermes,*[a] Christoph E. Sitta,[b] Burkhard Schillinger,[c] Hartmut Löwen[b] and Stefan U. Egelhaaf[a]

The dissolution of polyethylene oxide (PEO) tablets in water has been followed *in situ* by neutron radiography. When in contact with water, the crystalline phase of semi-crystalline PEO melts once a certain water content is attained. Polymer concentration profiles obtained from the neutron transmission images exhibited a pronounced kink which corresponds to a sharp front in the images and which is related to the melting transition. Sharp diffusion fronts and phase transitions are often linked to non-Fickian behaviour. However, by considering the time evolution of the complete concentration profiles in detail it is shown that the dissolution process can be explained using Fickian diffusion equations with a concentration-dependent diffusion coefficient.

Introduction

The transport of small molecules in polymeric materials has far reaching implications for such diverse problems as packaging,[1] food processing[2,3] and drug delivery.[4] Such movement can be quantified using diffusion equations and material-dependent diffusion coefficients. If two species are present in a system, a single mutual diffusion coefficient can be used.[5] For an initial concentration gradient, for example when two materials such as a polymer and a solvent come in contact, Fick's laws predict how the concentration gradient evolves with time.[5] These equations are widely applied and it is often assumed that the diffusion coefficient, D, is constant throughout the diffusion process. For a localised initial concentration and in the absence of outer boundary conditions, the molecules then spread within time t over a distance, l, as follows:

$$l^2 \propto Dt \tag{1}$$

Thus, experimental data are often plotted as l^2 against time, t, and the slope is taken to be proportional to the diffusion coefficient, D.[6] Frequently, if a non-linear relationship between l^2 and t is observed, the process is described as "non-Fickian". Modifications of Fick's laws have been suggested to describe such deviations.[5] For polymer systems, the term "Case II" was introduced very early to describe the dissolution behaviour of glassy polymers for which $l \propto t$ and a sharp penetration front are often reported.[7] It was proposed that the observed behaviour was unlikely to be explainable using concentration-dependent diffusion coefficients[7] and this belief has been propagated. Based on further experimental observations, a "non-Fickian model" was later developed[8] which has been popular and extended since.[9]

The most general way to obtain information on a diffusion process is to determine and analyse the time evolution of the spatially resolved concentrations, *i.e.* the concentration profiles.[5,9,12] Often, in quiescent, *i.e.* non-stirred, polymer–solvent systems, such profiles extend over hundreds of microns or more. Hence, quantitative experimental measurements must yield concentration values with spatial resolutions of (tens of) micrometers and temporal resolutions of seconds for centimetre-sized samples. By exploiting the neutron attenuation contrast between hydrogen and deuterium, such information can now be obtained for a wide range of materials by high flux neutron radiography, *i.e.* neutron transmission imaging, with modern scintillator-camera combinations. Other non-destructive profiling techniques such as magnetic resonance imaging,[6,13] infra-red imaging,[4,10] interferometry[11] and X-ray tomography[12] have been used to investigate *in situ* the diffusion of liquids in such materials[9] and these methods are all capable of yielding solvent concentration profiles as a function of time. However, experimental limitations of these more widely available techniques mean that in bulk samples they currently cannot fulfil all requirements simultaneously or require samples labelled with large atoms such as bromine.

[a] *Condensed Matter Physics Laboratory, Heinrich Heine University, D-40225 Düsseldorf, Germany. E-mail: helen.hermes@uni-duesseldorf.de*
[b] *Institute for Theoretical Physics II: Soft Matter, Heinrich Heine University, D-40225 Düsseldorf, Germany*
[c] *Heinz Maier-Leibnitz Zentrum (FRM II), Technische Universität München, D-85748 Garching, Germany*

This journal is © the Owner Societies 2015

Phys. Chem. Chem. Phys., 2015, **17**, 15781–15787 | 15781

Semi-crystalline poly(ethylene oxide) (PEO) is frequently used as a model substance for drug delivery including tablet dissolution[4,6,10,13] and is also of more fundamental interest.[14,15] Here we consider the diffusion of solvent molecules into and through a PEO matrix and the corresponding change in polymer concentration which occurs during the dissolution of a PEO tablet. The time evolution of concentration profiles is analysed using diffusion equations and diffusion coefficients with different concentration dependencies are determined.

Methods

Materials

Deuterium oxide (D_2O) with a purity of 99.9% was purchased from Deutero GmbH, Germany. PEO powders with nominal molar masses of 8×10^6 g mol^{-1} (Cat. No. 372838) and 1×10^5 g mol^{-1} (Cat. No. 18,198-6) were purchased from Aldrich. All materials were used as received. Discs 0.5 mm thick and nominal 4 mm in diameter were pressed using a simple cylinder and plunger device placed on a hot plate (temperatures above 65 °C) before being cooled to room temperature by placing them on a large metal block. At room temperature PEO is well above its glass transition temperature (which is generally quoted as lower than −40 °C) but below its melting temperature of about 65 °C and thus semi-crystalline when dry. PEO's degree of crystallinity is relatively independent of cooling rates, so that we expect between 50 and 75% of the dry material to be crystalline.[10] Three samples were measured, one with a nominal molar mass of 1×10^5 g mol^{-1}, denoted as "low", and two with a nominal molar mass of 8×10^6 g mol^{-1} denoted as "high1" and "high2". Although prepared in a similar manner, the two "high" samples differed in appearance: "high1" had a smooth, opal appearance whereas "high2" was partially white suggesting some inhomogeneity. Differences in appearance may be linked to differences in crystallinity and the presence of small voids.

Neutron radiography (NR)

NR measurements were performed on the ANTARES instrument at FRM II (München, Germany),[16] which offers the high collimation ratio (*i.e.* very parallel neutron beam) and neutron intensity required for our measurements. The sample were placed sufficiently close to the scintillator that the spatial resolution was limited by the detection set-up to approximately 50 μm. The image time and thus time resolution were chosen to be 60 s. During this time no structural detail moved further than the spatial resolution. Thus, smearing of the concentration profiles was avoided while sufficiently good neutron statistics were obtained.

The samples were held in aluminium cells with a fixed sample thickness, $d = 0.51$ (±0.02) mm, and thin integrated 20 mm diameter aluminium windows which were almost transparent to neutrons (Fig. 1a). The sample cell was held vertically in a thermostatted holder (Fig. 1b) and the temperature was maintained at 20 °C throughout the measurements. Due to the good thermal contact with the temperature-controlled block and the small temperature difference to room temperature, temperature gradients across the sample are not expected. Water was injected remotely into the cell through the tube visible in Fig. 1b and the overflow was collected in a syringe, which also acted as a reservoir. Several neutron images of the sample were collected before and during the water injection process so that the time at which the sample was first in contact with water could be determined.

The data were corrected pixel-wise for the background, detector efficiency and beam inhomogeneities and normalised to a reference area (solvent), which does not change during the experiment. This corrects for fluctuations in the incoming beam intensity and beam attenuation by the sample windows and yields a neutron transmission relative to the solvent, T_{rel}, for each pixel. The data were subsequently azimuthally averaged. The T_{rel} profiles thus obtained were converted to a polymer volume fraction, ϕ, as a function of distance to the centre of the tablet, r, *i.e.* to the concentration profile, assuming only polymer and water in the system and using the effective size of a pixel (16.0 μm) and the exponential law of attenuation for radiation which yields:

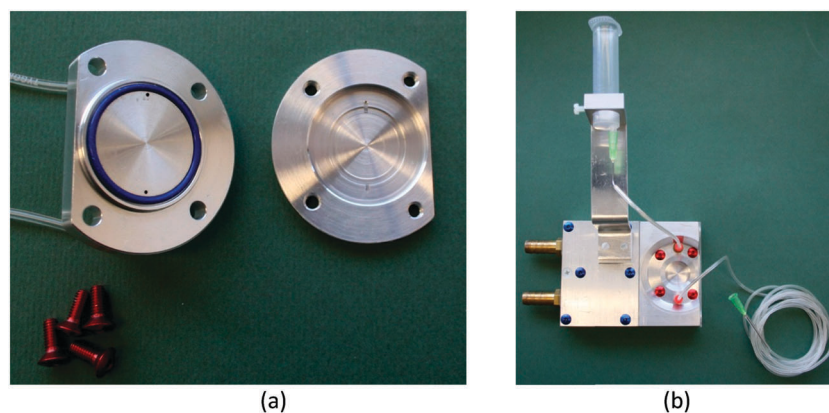$$\phi = \frac{\ln T_{rel}}{d(S_D - S_P)} \tag{2}$$

Fig. 1 (a) The two parts of the aluminium sample cell with integrated aluminium windows and (b) the temperature controlled sample cell holder with the sample cell in place and the inlet and overflow tubes for the solvent connected.

15782 | *Phys. Chem. Chem. Phys.*, 2015, **17**, 15781–15787

This journal is © the Owner Societies 2015

where S_P and S_D are the neutron absorption coefficients of the PEO matrix and D_2O, respectively.

Neutron absorption coefficients depend on the neutron wavelength, the detection system and other experimental details such as sample density and impurities. For our experimental situation we extracted experimental values for "low" of $dS_D = 0.034$, for "high1" of $dS_D = 0.038$ and for "high2" of $dS_D = 0.033$. Similarly, for polymer concentrations higher than the melting transition, we found experimental values for "low" of $dS_P = 0.206$, for "high1" of $dS_P = 0.257$ and for "high2" of $dS_P = 0.220$. These variations are expected to reflect the presence of voids in "high2" consistent with its white appearance together with differences in the degree of crystallinity and the sample thickness, d. At polymer concentrations lower than the melting transition (the kink in the profiles), values for "low" of $dS_P = 0.266$, for "high1" of $dS_P = 0.290$ and for "high2" of $dS_P = 0.289$ were estimated based on the change in density[17] and our experimental values at high polymer concentrations. The conversion must assume a sharp change in density at the melting transition. For "low" this was observed at $T_{rel} = 0.915$ *i.e.* $\phi \approx 0.5$, for "high1" at $T_{rel} = 0.900$ *i.e.* $\phi \approx 0.4$ and for "high2" at $T_{rel} = 0.915$ *i.e.* $\phi \approx 0.5$. Again, these variations are consistent with the presence of voids and differences in the degree of crystallinity. Together with uncertainties in the estimated value for S_P at high water concentrations, at the kink the assumed sharp change in density results in an expected relative error in ϕ of less than 5%. For other concentrations, the relative error in the volume fraction is expected to be nearer 1%. Errors in differences in time are significantly less than 1 s.

Calculations

Based on the experimental concentration profiles, the mutual diffusion coefficients as a function of concentration, $D(\phi)$, were determined using the 4 models described below. Experimental data from the centre of the tablet (innermost 0.38 mm, where few data points were available) were excluded from the fits due to poor statistics. The concentration profile when the polymer was first contacted with water, $t = 0$ s, was used as a starting profile for the calculations. The field of view was chosen to be sufficiently large to ensure that no polymer reaches the edge, *i.e.* $\phi = 0$ at the edge for all relevant times.

The top and bottom surfaces of the PEO tablets were not accessible to water resulting in a quasi two-dimensional geometry. Thus, the time evolution of the concentration profile, $\phi(r,t)$, is described by the two-dimensional diffusion eqn (5):

$$\frac{\partial \phi(r,t)}{\partial t} = D(\phi(r,t))\frac{\partial^2 \phi(r,t)}{\partial r^2} + \frac{\partial D(\phi(r,t))}{\partial r}\frac{\partial \phi(r,t)}{\partial r}$$
$$+ \frac{1}{r}D(\phi(r,t))\frac{\partial \phi(r,t)}{\partial r} \tag{3}$$

In this work it was implemented using an implicit finite difference scheme, which leads to a tri-diagonal set of linear equations. This was solved for each time step on a grid with a spacing of 12.7 μm which is less than the experimental resolution. This grid spacing yielded good spatial resolution, no divergence

and an acceptable computation time. As discussed in more detail in the Results section, the resulting $\phi(r,t)$ profiles were fit to the experimental data using the following four models for $D(\phi)$:

Model 1: constant D

$$D(\phi) = D_c \quad \text{Fit parameter}: D_c \tag{4}$$

Model 2: step change in D

$$D(\phi) = \begin{cases} D_1, & \phi \leq \phi_0 \\ D_2, & \phi > \phi_0 \end{cases} \quad \text{Fit parameters}: D_1, D_2, \phi_0 \tag{5}$$

Model 3: linear increase in D at low polymer concentrations and exponential decrease in D at high polymer concentrations

$$D(\phi) = \begin{cases} D_1(1+k\phi), & \phi \leq \phi_0 \\ D_2 e^{-\phi/\phi_c}, & \phi > \phi_0 \end{cases} \quad \text{Fit parameters}: D_1, D_2, k, \phi_c, \phi_0$$
$$\tag{6}$$

Model 4: 20 independently fit values for D for specific concentration ranges

$$D(\phi) = D_i \qquad \text{Fit parameters}: D_i$$
$$0.05(i-1) < \phi \leq 0.05i \quad i \in \{1, 2, 3, \ldots, 20\} \tag{7}$$

The fit parameters were not restricted except for physically reasonable ranges. Namely, the diffusion coefficients and slope k were forced to be non-negative and the volume fractions to be in the range 0 to 1.

Results and discussion

Using neutron radiography, the dissolution of a polyethylene oxide (PEO) tablet in water was followed *in situ* for 3 samples: "low" $(1 \times 10^5 \text{ g mol}^{-1})$, "high1" and "high2" (both $8 \times 10^6 \text{ g mol}^{-1}$). The top and bottom surfaces of the PEO tablets were not accessible to water resulting in a quasi two dimensional geometry. The neutron transmission images (Fig. 2a–d) revealed one rather sharp front corresponding to water moving into the dry PEO tablet and a less well defined swelling front moving out into the bulk liquid. From the images, the transmission profiles as a function of time t, $T_{rel}(r,t)$, were extracted and subsequently converted to polymer concentration profiles, $\phi(r,t)$, where r is the distance to the tablet centre (Fig. 2e, f). Qualitatively, the general shapes of all profiles from all samples were similar and exhibited a distinct kink at about the same transmission, *i.e.* polymer concentration. This corresponds to the sharp front seen in the images and can be attributed to the melting transition of the PEO at this concentration caused by the increase in solvent content. Sharp diffusion fronts and phase transitions have often been linked to non-Fickian behaviour.[5,18]

The relationship between l^2 and t is often used to indicate the prevailing diffusional behaviour in a system. Typically, in (optical) transmission experiments, a front position L which is associated with a particular concentration or a concentration step is taken to be equivalent to l (eqn (1)). However, since the shape of the diffusion front usually changes with time, mere consideration of one feature of the front, such as a specific
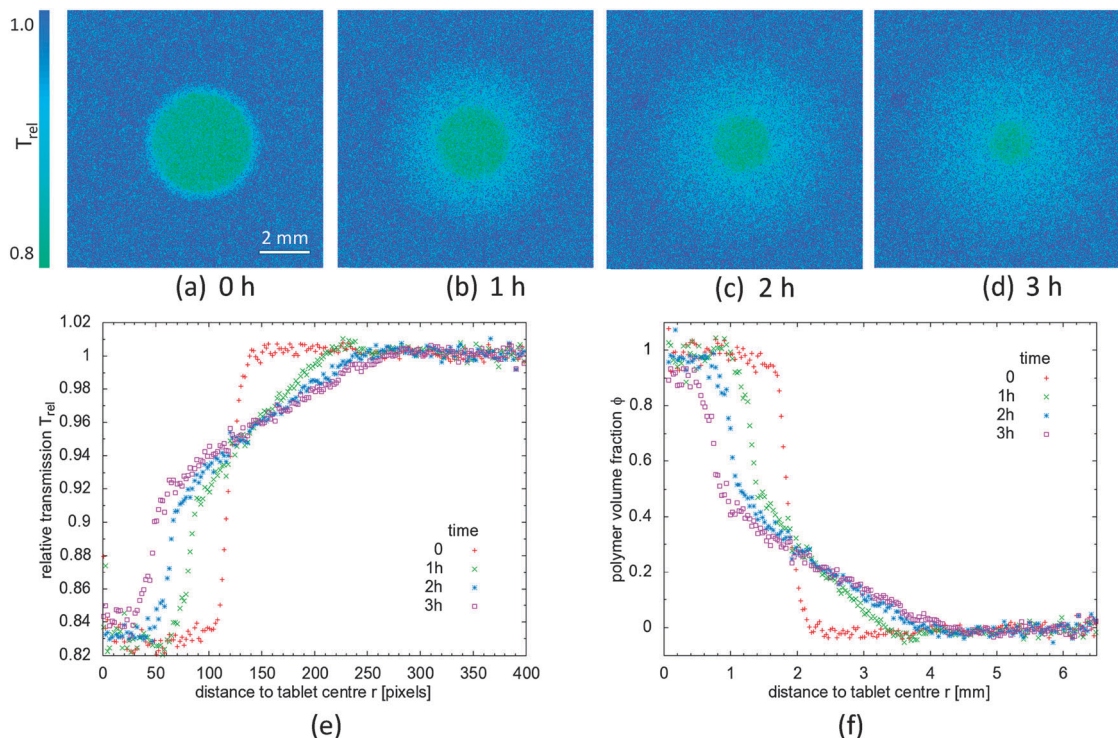
This journal is © the Owner Societies 2015

Phys. Chem. Chem. Phys., 2015, **17**, 15781–15787 | **15783**

Fig. 2 (a−d) Representative neutron radiography transmission images of a semi-crystalline PEO tablet (sample ''high2'') in contact with water at different times and the corresponding (e) transmission and (f) concentration profiles extracted from these (times as indicated).

concentration or concentration step, results in the introduction of an arbitrary criterion and the recording and exploitation of limited information. To illustrate this, for a two-dimensional radial geometry and an initial sharp concentration step profile, we used Fick's equations and a constant diffusion coefficient to calculate the development of the concentration profiles (Methods). Even for this simple situation, tracking the positions of several concentrations, *i.e.* possible "fronts", shows that the relationship between L^2 and t depends on the concentration selected and is not linear over an extended time range (Fig. 3a). Hence, a non-linear relationship between L^2 and t does not necessarily imply that

Fick's laws do not apply, *i.e.* that the diffusional behaviour is ''non-Fickian''. To test whether our experimental data could be described by a constant diffusion coefficient, D_c, we repeated the procedure using the experimental initial profile as the starting point (Fig. 3b, solid lines). For only one concentration (indicated in red), the calculated position seems to agree reasonably well with the data for the first few hours. This is however not the case for the other concentrations. Thus, analysis of the complete concentration profiles is crucial.

In the calculations above, we considered a constant diffusion coefficient. Where only a small change in concentration and no
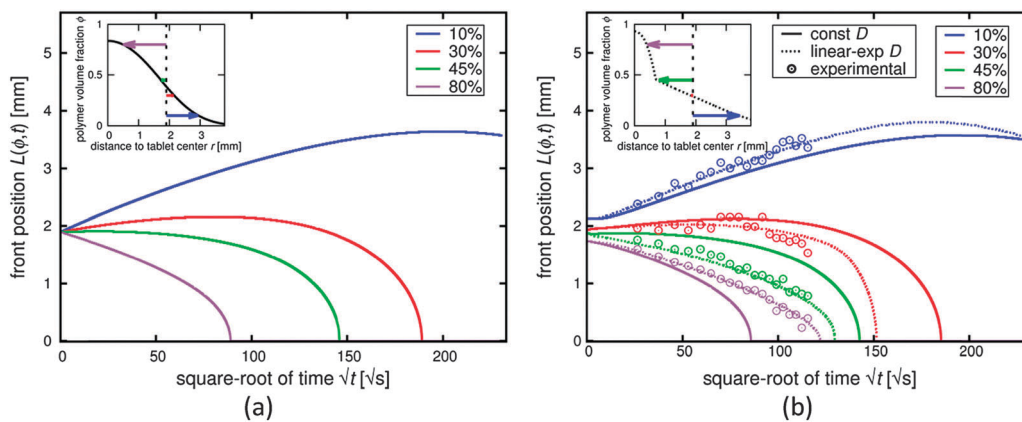

Fig. 3 Time dependence of four concentrations ϕ_L (as indicated and illustrated in the insets for a typical profile) as calculated based on Fick's laws for (a) a constant diffusion coefficient and an initially sharp concentration profile and (b) a constant (solid lines) and a concentration-dependent (Model 3, dotted lines) diffusion coefficient and the initial experimental profile. The latter are compared to the corresponding experimental data (symbols; sample ''high2'').

15784 | *Phys. Chem. Chem. Phys.,* 2015, **17**, 15781–15787

This journal is © the Owner Societies 2015

structural changes occur, the assumption of a constant diffusion coefficient may be reasonable. However, the large changes in concentration which occur during dissolution or during the mixing of two species are typically accompanied by considerable changes in the diffusion coefficient.[19] In addition, polymers which exhibit a semi-crystalline morphology such as PEO contain a compact crystalline phase which has a low permeability.[10,20] Once solvent penetrates this phase, it causes it to melt and become more permeable.[10] Due to this pronounced change in permeability, the melting transition is anticipated to cause a significant change in the diffusion coefficient. On a molecular scale, such concentration dependence of the diffusion coefficient incorporates all the effects of reptation, free volume, etc.[9,18]

To quantitatively analyse our concentration profiles, we used the appropriate 2-D diffusion equations (eqn (3)). Not surprisingly, the concentration profiles could not be described using a constant diffusion coefficient (eqn (4); Fig. 4, solid line). Thus, we considered the concentration dependence of the diffusion coefficient. For 1-D systems, the concentration dependence of the diffusion coefficient, $D(\phi)$, can be extracted directly from the concentration profile using the Boltzmann–Matano method which is based on $c(x,t) = c(x/t^{0.5})$.[5] However, for radial geometry, scaling onto a single variable is impossible. Hence, we used three increasingly complex models to describe $D(\phi)$ (eqn (5)–(7)). All three relationships were able to reproduce the kink seen in the experimental concentration profiles. The simplest, a step model, describes $D(\phi)$ using two values which are both constant for a certain concentration range – one each for concentrations above and below the melting transition, ϕ_0 (eqn (5)). It fits the data reasonably well (Fig. 4, dash-dotted line). However, the diffusion coefficient is not likely to remain constant over a large concentration range so that this model oversimplifies the situation and is not physically accurate. The concentration dependence within the two concentration regimes is taken into account in the next approach in which we assume for $D(\phi)$ a

linear dependence for polymer solutions, as found previously using other experimental techniques,[21,22] and an exponential drop in the partially crystalline polymer, as suggested for other low solvent content systems[5,8] (eqn (6)). Agreement with the concentration profiles was indeed improved (Fig. 4, dotted line). In addition, experimentally determined and calculated positions of specific concentrations, L, agree for the entire measurement (Fig. 3b). Finally, in the last approach, no specific relationship was assumed *a priori* for $D(\phi)$ and 20 values each covering 5% in composition were fitted to the data (eqn (7)). Agreement between the calculated and experimental profiles was comparable to that found for the previous approach and can be barely differentiated in Fig. 4 (dotted *vs.* dashed lines). Also, the shape of $D(\phi)$ obtained was similar except that the transition at the melting composition was broader. A continuous rather than discrete transition in $D(\phi)$ at the melting transition is reasonable since polymer melting transitions are generally broad. The form of $D(\phi)$ which we extracted from the experimental concentration profiles agrees with expected trends and can be understood in terms of changes in permeability with concentration combined with a significant change at the melting transition. The absolute values correlate broadly with values of $D(\phi)$ for limited concentration ranges in the literature.[21,22]

The above discussion concentrates on sample "high2" for which most data (times) are available. The images and profiles obtained for a second large molar mass sample, "high1", were very similar. We also investigated PEO with a lower molar mass, "low". Ingress of water into this tablet was isotropic as in both "high" tablets. By contrast, for this sample, swelling of the dissolved PEO into the solution was not isotropic but appeared to be affected by gravity, *i.e.*, the vertical position of the sample. Thus, analysis of those parts of the profiles corresponding to the solution phase was impossible for the "low" sample, and $D(\phi)$ could only be obtained within the tablet. A horizontal geometry is not feasible due to the horizontal nature of the neutron beam.
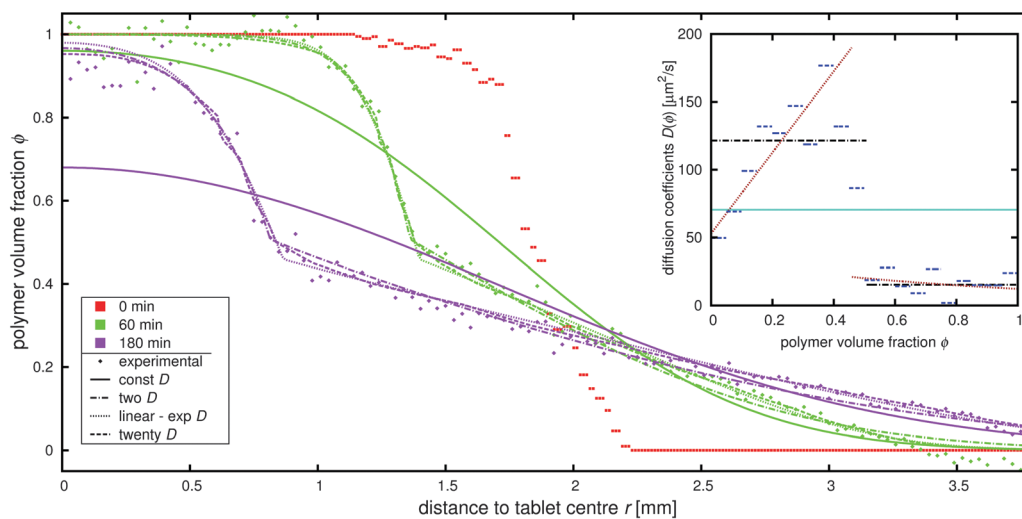

Fig. 4 Experimentally observed concentration profiles (symbols; sample "high2") and the corresponding fits for the four models describing the concentration-dependence of the diffusion coefficient. (Solid line: constant diffusion coefficient, dash-dotted line: two-value diffusion coefficient, dotted line: linear-exponential model, and dashed line: "twenty D" model.) Inset: fitted $D(\phi)$ for the four models with the corresponding line styles.
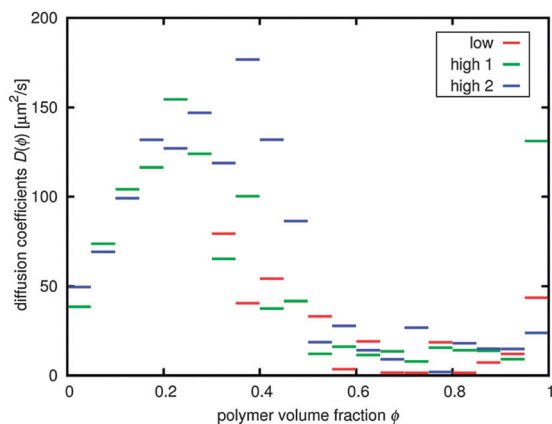
Fig. 5 Comparison of $D(\phi)$ obtained using the "twenty D" model (eqn (7)) for the three samples studied. No results are shown for sample "low" at low polymer volume fractions because its anisotropic swelling (due to the vertical sample position) made analysis impossible.

All modelling approaches (eqn (4) to (7)) were applied to all three samples and found to yield similar results. Fig. 5 compares the results obtained for the "twenty D" model (eqn (7)). For all three samples, $D(\phi)$ is similar at high polymer volume fractions. This suggests that for these concentrations, diffusion is limited by the crystalline phase irrespective of the polymer molar mass. At low polymer volume fractions, $D(\phi)$ for "high1" and "high2" agree which is also expected as these samples have the same molar mass. As mentioned above, data for "low" could not be determined at low concentrations. At intermediate polymer volume fractions, around the kink in the profiles, there is some difference in $D(\phi)$. This is likely to be due to differences in the dynamic melting behaviour due to the presence of voids as well as possible differences in the degree of crystallinity.

Conclusions

The time evolution of concentration profiles during the dissolution of bulk semi-crystalline PEO has been determined *in situ* using neutron radiography. Combining the appropriate diffusion equation with a concentration-dependent diffusion coefficient, $D(\phi)$, we successfully described the time-dependence of the concentration profiles including the observed kink which is associated with an experimentally observed sharp diffusion front and a melting transition. We found no need to invoke "non-Fickian" behaviour. The concentration dependency of $D(\phi)$ found agreed with expected trends and the absolute values correlated broadly with values of $D(\phi)$ available in the literature for limited concentration ranges.[21,22] Our *in situ* dissolution measurements are appropriate for kinetic processes such as tablet dissolution. To our knowledge, $D(\phi)$ has not previously been determined for the PEO–water system for the entire concentration range.

Similar neutron imaging experiments and modelling considerations could be applied to other polymers and hence allow rigorous testing of more complicated models which have been proposed to describe the ingress of the solvent into such materials.[5,8,9] These models could previously only be checked indirectly *via* staining or increases in volume or mass, or for limited concentration or spatial ranges. The approach discussed, based on the novel application of neutron radiography combined with the concept of a concentration-dependent diffusion coefficient, is expected to be relevant for a wide range of applications in different materials including other soft and complex matter systems of both natural and synthetic origin.[23–26]

Acknowledgements

References

1 J.-W. Rhim, H.-M. Park and C.-S. Ha, Bio-nanocomposites for food packaging applications, *Prog. Polym. Sci.*, 2013, **38**, 1629–1652.
2 N. Yazdanpanah and T. A. G. Langrish, Mathematical modelling of the heat and moisture diffusion in a dairy powder particle with crystallisation phase change within the particle matrix, *Int. J. Heat Mass Transfer*, 2013, **61**, 615–626.
3 R. Mezzenga, P. Schurtenberger, A. Burbridge and M. Michel, Understanding foods as soft materials, *Nat. Mater.*, 2005, **4**, 729–740.
4 K. L. A. Chan and S. G. Kazarian, ATR-FTIR spectroscopic imaging with expanded field of view to study formulations and dissolution, *Lab Chip*, 2006, **6**, 864–870.
5 J. Crank, *The Mathematics of Diffusion*, Oxford University Press, 1975.
6 T. M. Hyde and L. F. Gladden, Simultaneous measurement of water and polymer concentration profiles during swelling of poly(ethylene oxide) using magnetic resonance imaging, *Polymer*, 1998, **39**, 811–819.
7 T. Alfrey, E. F. Gurnee and W. G. Lloyd, Diffusion in glassy polymers, *J. Polym. Sci., Part C: Polym. Symp.*, 1966, **12**, 259–261.
8 N. L. Thomas and A. H. Windle, A theory of Case II diffusion, *Polymer*, 1982, **23**, 529–542.
9 D. Vesely, Diffusion of liquids in polymers, *Int. Mater. Rev.*, 2008, **53**, 299–315.
10 C. Coutts-Lendon and J. L. Koenig, Investigation of the aqueous dissolution of semicrystalline poly(ethylene oxide) using infrared chemical imaging: The effects of molecular weight and crystallinity, *Appl. Spectrosc.*, 2005, **50**, 976–985.
11 J. Crank and C. Robinson, Interferometric studies in diffusion. II. Influence of concentration and orientation on diffusion in cellulose acetate, *Proc. R. Soc. London, Ser. A*, 1951, **204**, 549–569.
12 A. K. Ekenseair, R. A. Ketcham and N. A. Peppas, Visualization of anomalous penetrant transport in glassy poly(methyl methacrylate) utilizing high-resolution X-ray computed tomography, *Polymer*, 2012, **53**, 776–781.

15786 | *Phys. Chem. Chem. Phys.*, 2015, **17**, 15781–15787

This journal is © the Owner Societies 2015

13 S. Abrahmsén-Alami, A. Körner, I. Nilsson and A. Larsson, New release cell for NMR microimaging of tablets. Swelling and erosion of poly(ethylene oxide), *Int. J. Pharm.*, 2007, **342**, 105–114.

14 M. Brodeck, F. Alvarez, A. Arbe, F. Juranyi, T. Unruh, O. Holderer, J. Colmenero and D. Richter, Study of the dynamics of poly(ethylene oxide) by combining molecular dynamic simulations and neutron scattering experiments, *J. Chem. Phys.*, 2009, **130**, 094908.

15 C. Trotzig, S. Abrahmsén-Alami and F. H. J. Maurer, Structure and mobility in water plasticized poly(ethylene oxide), *Polymer*, 2007, **48**, 3294–3305.

16 B. Schillinger, E. Calzada and K. Lorenz, Modern neutron imaging: Radiography, tomography, dynamic and phase contrast imaging with neutrons, *Solid State Phenom.*, 2006, **112**, 61–72.

17 C. Sommer, J. S. Pedersen and P. C. Stein, Apparent specific volume measurements of poly(ethylene oxide), poly(butylene oxide), poly(propylene oxide) and octadecyl chains in the micellar state as a function of temperature, *J. Phys. Chem. B*, 2004, **108**, 6242–6249.

18 L. Masaro and X. X. Zhu, Physical models of diffusion for polymer solutions, gels and solids, *Prog. Polym. Sci.*, 1999, **24**, 731–775.

19 E. L. Cussler, *Diffusion: Mass transfer in fluid systems*, Cambridge University Press, 1985.

20 M. Laurati, P. Sotta, D. R. Long, L.-A. Fillot, A. Arbe, A. Alegrìa, J. P. Embs, T. Unruh, G. J. Schneider and J. Colmenero, Dynamics of water absorbed in polyamides, *Macromolecules*, 2012, **45**, 1676–1687.

21 C. Branca, A. Faraone, S. Magazù, G. Maisano, P. Migliardo and V. Villari, Polyethylene oxide: a review of experimental findings by spectroscopic techniques, *J. Mol. Liq.*, 2000, **87**, 21–68.

22 K. Devand and J. C. Selser, Asymptotic behaviour and long-range interactions in aqueous solutions of poly(ethylene oxide), *Macromolecules*, 1991, **24**, 5943–5947.

23 L. Nie, A. Burgess and A. Ryan, Moisture permeation in liquid crystalline epoxy thermosets, *Macromol. Chem. Phys.*, 2013, **214**, 225–235.

24 A. Furukawa and H. Tanaka, Dynamic scaling for anomalous transport in supercooled liquids, *Phys. Rev. E: Stat., Nonlinear, Soft Matter Phys.*, 2012, **86**, 030501(R).

25 B. Coasne, C. Alba-Simionesco, F. Audonnet, G. Dosseh and K. E. Gubbins, Adsorption, structure and dynamics of benzene in ordered and disordered porous carbon, *Phys. Chem. Chem. Phys.*, 2011, **13**, 3748–3757.

26 D. G. Bucknall, J. S. Higgins and S. A. Butler, Real-time neutron reflectivity study of the early stages of diffusion into and dissolution of glassy polymers, *J. Polym. Sci., Part B: Polym. Phys.*, 2004, **42**, 3267–3281.